Original Article

LINC01977 promotes colorectal cancer growth and metastasis by enhancing aerobic glycolysis via the ERK/c-Myc axis

Jie Wu[1#^], Qiwen Chen[2#], Yunliang Wang[3#], Ruoqin Wang[1], Qing Chen[4], Yuhan Wang[1], Xin Qi[5], Yuan Gao[1], Kai Chen[1]

[1]Department of Oncology, The First Affiliated Hospital of Soochow University, Suzhou, China; [2]Minimally Invasive Therapy Center, Department of Integrative Oncology, Fudan University Shanghai Cancer Center, Shanghai, China; [3]Department of General Surgery, The First Affiliated Hospital of Soochow University, Suzhou, China; [4]Department of Oncology, Jingjiang People's Hospital, The Seventh Affiliated Hospital of Yangzhou University, Jingjiang, China; [5]School of Chemistry and Life Sciences, Suzhou University of Science and Technology, Suzhou, China

Contributions: (I) Conception and design: K Chen, Y Gao, X Qi; (II) Administrative support: None; (III) Provision of study materials or patients: None; (IV) Collection and assembly of data: J Wu, Qiwen Chen; (V) Data analysis and interpretation: J Wu, Yunliang Wang; (VI) Manuscript writing: All authors; (VII) Final approval of manuscript: All authors.

[#]These authors contributed equally to this work.

Correspondence to: Kai Chen, MD, PhD; Yuan Gao, MD. Department of Oncology, The First Affiliated Hospital of Soochow University, No. 899 Pinghai Road, Suzhou 215006, China. Email: cky9920@163.com; yuangao01@126.com; Xin Qi, PhD. School of Chemistry and Life Sciences, Suzhou University of Science and Technology, No. 99 Xuefu Road, Suzhou 215011, China. Email: qixin@usts.edu.cn.

Background: How colorectal cancer (CRC) gain the ability to growth and metastasis remains largely unknown. Findings from preceding studies have revealed the participation of long non-coding RNAs (lncRNAs) in CRC progression. However, the role of LINC01977 in CRC remains unexplored. This study aims to explore the function and underlying mechanism of LINC01977 in CRC.

Methods: The Cancer Genome Atlas (TCGA) and Gene Expression Omnibus (GEO) datasets were used to analyze the expression of LINC01977 in CRC and its correlation with CRC prognosis. In our research, we explored the influence of LINC01977 on CRC progression such as cell proliferation, migration, invasion, and aerobic glycolysis, and identified its fundamental molecular mechanism using *in vitro* CRC cell lines and in vivo mouse xenograft models.

Results: LINC01977 exhibited significantly elevated expression in CRC tissues and cell lines, and its level was significantly correlated with malignant clinicopathological characteristics and negative prognosis. Furthermore, both *in vivo* and *in vitro* tests revealed LINC01977's role in facilitating CRC cell proliferation and metastasis. LINC01977's significant part in CRC aerobic glycolysis was also discovered. With an aim to uncover the underlying mechanism, we investigated LINC01977's effect on c-Myc, a key gene in glycolysis. The results showed that LINC01977 regulated c-Myc stability via extracellular signal-regulated kinase (ERK)-mediated phosphorylation, and LINC01977-mediated c-Myc activated the level of vital glycolysis-related genes such as *HK2*, *PGK1*, *LDHA*, and *GLUT1*. Rescue experiments further confirmed that LINC01977 promoted CRC proliferation, metastasis, and aerobic glycolysis via c-Myc.

Conclusions: This study is the first to report that LINC01977 facilitates CRC proliferation, metastasis, and aerobic glycolysis through c-Myc, suggesting its potential as a therapeutic target for CRC treatment.

Keywords: Colorectal cancer (CRC); LINC01977; glycolysis; c-Myc

Submitted Jan 18, 2024. Accepted for publication Feb 19, 2024. Published online Feb 28 2024.
doi: 10.21037/jgo-24-52
View this article at: https://dx.doi.org/10.21037/jgo-24-52

^ ORCID: 0000-0001-8141-9417.

Introduction

Globally, colorectal cancer (CRC) is acknowledged as the second leading cause of cancer-related deaths, causing approximately 1 million fatalities in 2020 (1). The incidence of CRC has been on the rise in countries with an increasing human development index, particularly among individuals below the age of 50 years (2). Although the implementation of CRC screening programs has led to higher rates of early detection, a significant number of CRC patients still receive diagnoses at advanced stages, often missing opportunities for potentially curative resection (3). Despite the notable advancements made, the existing therapeutic strategies and survival advantages for progressive CRC are currently limited. Consequently, there is an urgent need for research into novel biomarkers and targets to enhance the outcomes of CRC.

Long non-coding RNAs (lncRNAs) represent a class of non-coding transcript that are longer than 200 nucleotides. Extensive studies have shown the disruption of lncRNAs in various forms of cancer, such as CRC, emphasizing their crucial involvement in promoting the advancement of cancer (4-7). However, the functions of the majority of lncRNAs in CRC have yet to be characterized. Therefore, it is essential to identify lncRNAs associated with CRC for subsequent functional validation. LINC01977 has been reported to facilitate the progression of lung adenocarcinoma, breast cancer, and hepatocellular carcinoma (8-10), yet its role in CRC has not been previously. In this study, our investigations revealed increased expression of LINC01977 in CRC, which correlates with a poor prognosis in patients. Through functional analyses, we demonstrated that LINC01977 plays a critical oncogenic role in CRC by promoting its growth and metastasis. As a result, our findings shed light on the potential mechanisms and clinical implications of LINC01977 in CRC, providing fresh perspectives into the development of this condition. We present this article in accordance with the ARRIVE and MDAR reporting checklists (available at https://jgo.amegroups.com/article/view/10.21037/jgo-24-52/rc).

Highlight box

Key findings

- We reported that LINC01977 facilitates colorectal cancer (CRC) proliferation, metastasis, and aerobic glycolysis through c-Myc.

What is known and what is new?

- LINC01977 exhibited significantly elevated expression in CRC, correlated with malignant clinicopathological characteristics and negative prognosis.
- LINC01977 regulated c-Myc stability via extracellular signal-regulated kinase (ERK)-mediated phosphorylation, facilitated CRC cell proliferation and metastasis.

What is the implication, and what should change now?

- This study may provide new insights into how aerobic glycolysis affects colorectal cancer cell growth and metastasis, which may provide new ideas and insights into individualized treatment of colorectal cancer patients.

Methods

The Cancer Genome Atlas (TCGA) and Gene Expression Omnibus (GEO) data analysis

RNA expression data (Level 3) for patients with CRC and associated clinical information were acquired from TCGA (https://portal.gdc.cancer.gov/). The obtained results were then analyzed and visualized using R 3.6.3 (The R Foundation for Statistical computing, Vienna, Austria). Analysis was conducted using data collection and data processing of the LINC01977-associated datasets in GEO (http://www.ncbi.nlm.nih.gov/geo).

Clinical samples

Primary human CRC tissues from 38 patients, coupled with corresponding noncancerous tissues, were procured from the First Affiliated Hospital of Soochow University in 2022. The patients who underwent tumor resection had not undergone neoadjuvant chemoradiotherapy, including at the onset of treatment following diagnosis. Tissue samples were quickly frozen in liquid nitrogen after tumor removal and then stored at –80 ℃ for the extraction of total RNA. The study was conducted in accordance with the Declaration of Helsinki (as revised in 2013). The study was approved by the Ethics Committee of the First Affiliated Hospital of Soochow University (No. 2022344) and informed consent was taken from all the patients.

Cell lines culture

The human CRC cell lines HCT116, HT29, KM12, LoVo, SW620, SW480, RKO, and HEK-293T and the human normal colon epithelial cell line NCM460 were obtained from the Cell Bank of the Chinese Academy of Sciences (Shanghai, China) and the American Type Culture Collection (ATCC; Manassas, VA, USA). Cells

were cultured in either Dulbecco's modified Eagle medium (DMEM; Cat # SH30022; HyClone, Logan, UT, USA) or Roswell Park Memorial Institute (RPMI) 1640 medium (Cat # SH30809, HyClone), with the addition of 10% fetal bovine serum (FBS; Cat # 10100147, Gibco, Waltham, MA, USA) to both DMEM and RPMI 1640 medium. The cell cultures were kept in a CO_2 incubator (5% CO_2) at a temperature of 37 ℃.

Cell transfection and plasmids

The antisense oligonucleotide (ASO) against human LINC01977 and a control ASO were synthesized from RiboBio (Guangzhou, China). The pCDH-EF1-MCS-CMV-copGFP-T2A-Puro, pCDH-EF1-LINC01977-CMV-copGFP-T2A-Puro, pCDH-EF1-c-Myc-CMV-copGFP-T2A-Puro, pLKO.1-shCtrl, and pLKO.1-shLINC01977 plasmids were constructed from Logen Biotechnology (Suzhou, China). For the production of lentiviral particles in HEK-293T cells, the plasmids were cotransfected with psPAX2 and pMD2.G helper plasmids. The transfection of ASO and the plasmids was completed in line with the producer's protocol, using Lipofectamine 3000 reagent (Cat # 100022052; Invitrogen, Carlsbad, CA, USA).

RNA extraction and quantitative real-time polymerase chain reaction

Based on the manufacturer's directions, a TRIzol reagent kit (Cat # 1559601, Invitrogen) was used for RNA extraction from tissues or cells. The All-In-One RT MasterMix kit [Cat # G592; Applied Biological Materials (ABM), Richmond, British Colombia, Canada] was used for reverse transcription; quantitative real-time polymerase chain reaction (qRT-PCR) was performed using qPCR Master Mix (Cat # G890, ABM) according to the supplier's guidelines with β-actin as a control. The primer sets used were listed as follows: LINC01977: 5'-GTCTAACGCAGGGGGAAACA-3' (forward), 5'-TATTGCCAACAACTGGCCCT-3' (reverse); HK2: 5'-GATTGTCCGTAACATTCTCATCGA-3' (forward), 5'-TTGTCTTGAGCCGCTCTGAGATG-3' (reverse); PGK1:5'-TCACTCGGGCTAAGCAGATT-3' (forward), 5'-CAGTGCTCACATGGCTGACT-3' (reverse); LDHA: 5'-GATTCCAGTGTGCCTGTATGGAGT-3' (forward), 5'-CACCTCATAAGCACTCTCAACCACC-3' (reverse); GLUT1: 5'-GAGCAGCTACCCTGGATGTCCTA-3' (forward), 5'-CACATACTGGAAGCACATGCCCAC-3' (reverse); β-actin: 5'-CTCACCATGGATGATGATATCGC-3' (forward); 5'-AGGAATCCTTCTGACCCATGC-3' (reverse).

Assays for cell proliferation and the formation of colonies

The viability of the cells was evaluated using a cell counting kit-8 (CCK-8; Cat # C0038; Beyotime, Shanghai, China) according to the instructions provided by the supplier. To perform the colony formation test, approximately 1,000 cells were placed into every well of 6-well plates, and incubated in a medium containing 10% FBS (Cat # 10100147, Gibco) for a period of 12 days until colonies became visible. Afterwards, the colonies were treated with paraformaldehyde (Cat # P0099, Beyotime) and stained using 0.1% crystal violet (Cat # C0121, Beyotime), following which the number of colonies was determined.

Scratch wound healing assay

The cells were seeded onto 24-well dishes and incubated until they formed a cohesive layer, a wound was created by using a 10 µL pipette tip, and then the wells were washed with a culture medium to remove any detached cells. Images of the wound area were captured at 0 and 24 h, and the percentage of wound closure compared to the initial size was calculated via using the ImageJ software (National Institutes of Health, Bethesda, MD, USA).

Transwell assay

Around 1×10^5 cells were introduced into the upper section of the transwell chamber (Cat # 3422, Corning, NY, USA). These cells were then cultured with 100 µL of medium without serum in the upper section, and the lower chamber contained 600 µL of complete medium. Following a 48-hour incubation period, the cells on the underside were treated with 4% paraformaldehyde (Cat # P0099, Beyotime) for 30 min and subsequently subjected to staining with 0.1% crystal violet (Cat # C0121, Beyotime) prior to microscopic examination. For the experiments in the transwell invasion assay, the transwell chamber was pre-coated with Matrigel [Cat # 356234; Becton, Dickinson, and Co. (BD) Biosciences, Franklin Lakes, NJ, USA].

Animal experiments

Shanghai Laboratory Animal Center (SLAC; Shanghai,

China) provided BALB/c-nu mice (20 g, female, 5 weeks old) housed in filter-capped microisolator cages, along with sterilized food and water for the animals. In the xenograft tumor experiment, the mice were randomly divided into 4 groups (HCT116-Ctrl, HCT116-LINC01977, SW620-shCtrl, and SW620-shLINC01977) with 6 mice in each group, and phosphate-buffered saline (PBS; Cat # C0221A, Beyotime) was used to suspend a total of 4×10^6 cells (HCT116-Ctrl, HCT116-LINC01977, SW620-shCtrl, or SW620-shLINC01977 cells), which were then injected subcutaneously into the backs of the mice to establish the xenograft tumors. The size of the tumor was measured twice every week, for 4 weeks after the implantation. Subsequently, the mice were euthanized, and the tumor mass was extracted, weighed, and assessed for its volume. In the lung metastasis experiment, the mice were randomly divided into 4 groups (HCT116-Ctrl, HCT116-LINC01977, SW620-shCtrl, and SW620-shLINC01977) and were injected with 2×10^6 cells (HCT116-Ctrl, HCT116-LINC01977, SW620-shCtrl, or SW620-shLINC01977 cells) through the tail vein. After 4 weeks, the mice were euthanized, and the lung tissues were dissected and preserved in a 10% neutral buffered formalin solution (Cat # HT501128; Merck, Rahway, NJ, USA). Metastatic foci in lung tissue were tallied on hematoxylin and eosin (H&E)-stained slides. Animal experiments were performed under a project license (No. 2021243) granted by the Animal Ethics Committee of the First Affiliated Hospital of Soochow University, in compliance with Chinese National Standard (GBT35823-2018) for the care and use of animals. A protocol was prepared before the study without registration.

Glucose uptake, lactate production, and ECAR assay

The Glucose Assay Kit (Cat # F006-1-1; Jiancheng Bioengineering Institute, Nanjing, China) and the Lactate Assay Kit (Cat # A019-2, Jiancheng) were used to conduct glucose uptake and lactate production assays, respectively, in accordance with the manufacturer's instructions. The glycolytic process was evaluated using an extracellular acidification rate (ECAR) assay, and the Seahorse Bioscience XF96 Extracellular Flux Analyzer was utilized according to the instructions given with the Seahorse XF Glycolysis Stress Test Kit (Cat # 103020-100; Seahorse Bioscience, Billerica, MA, USA) to determine the cellular glycolytic capacity.

Western blot analysis

Proteins from the samples were extracted using radioimmunoprecipitation assay (RIPA) lysis buffer (Cat # R0278, Merck), and the protein concentration in lysates were measured by bicinchoninic acid (BCA) assay (Cat # P0010S, Beyotime). The proteins were separated based on their molecular weight using sodium dodecyl sulfate polyacrylamide gel electrophoresis (SDS-PAGE; Cat # P0012AC, Beyotime), and the separated proteins were transferred from the gel onto a polyvinylidene fluoride (PVDF) membrane (Cat # IPVH00010; Merck Millipore, Burlington, MA, USA) using electroblotting. The non-specific binding sites on the membrane were blocked by incubating with 5% non-fat milk, then the membrane was incubated with a primary antibody at 4 ℃ overnight. The membrane was then incubated with a secondary antibody (the anti-rabbit or anti-mouse antibodies) at 25 ℃ for 2 hours. Electrochemiluminescence (ECL; Cat # P0018M, Beyotime) detection method was used to visualize the protein bands. The primary antibodies included anti-HK2 (Cat # 66974-1-Ig; Proteintech, Rosemont, IL, USA) (1:1,000), anti-PGK1 (Cat # 17811-1-AP, Proteintech) (1:1,000), anti-LDHA (Cat # 66287-1-Ig, Proteintech) (1:1500), anti-GLUT1 (Cat # 66290-1-Ig, Proteintech) (1:1,500), anti-β-actin (Cat # sc-47778; Santa Cruz Biotechnology, Santa Cruz, CA, USA) (1:1,000), anti-ERK [Cat # 9102; Cell Signaling Technology (CST), Danvers, MA, USA] (1:1,000), anti-p-ERK (Cat # 9101, CST) (1:1,000), anti-pS62-c-Myc (Cat # 13748, CST) (1:1,500), and anti-c-Myc (Cat # 9402, CST) (1:1,000).

Statistical analysis

Each experiment was performed at least 3 times, and differences between groups were examined by applying one-way analysis of variance (ANOVA) or independent paired *t*-tests (2-tailed) using GraphPad Prism 7.0 (GraphPad Software, San Diego, CA, USA) or SPSS 24.0 (IBM Corp., Armonk, NY, USA) for statistical analysis. Significant differences were deemed at $P<0.05$.

Results

Increased expression of LINC01977 in CRC

At first, comprehensive analyses across different types of cancer showed that LINC01977 displayed elevated levels

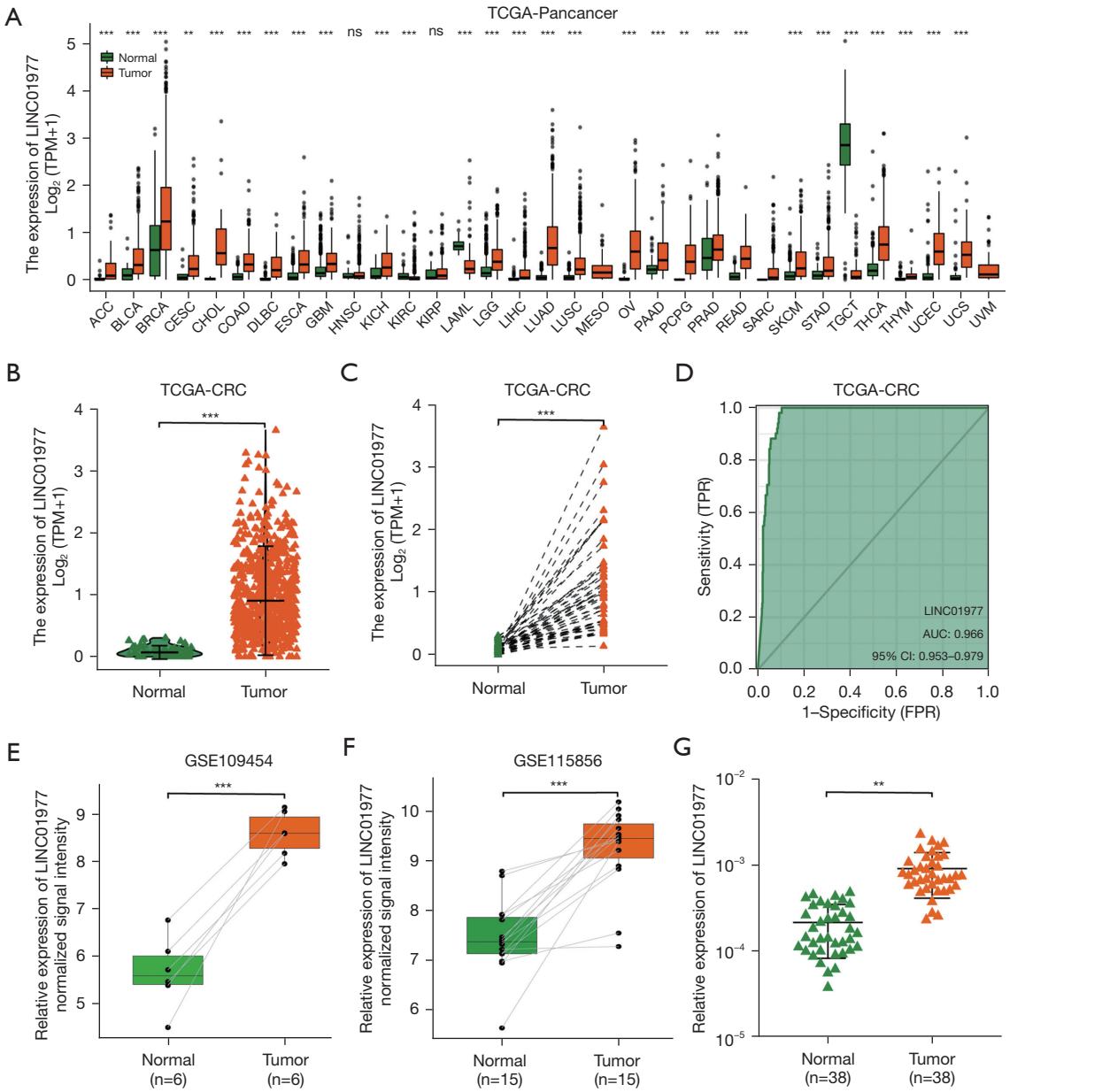

Figure 1 Variations in the expression levels of LINC01977 in various malignancies and CRC. (A) Comparing the expression of LINC01977 in tumors and normal tissues across various cancer types using the TCGA database. (B) The expression of LINC01977 in CRC and surrounding tissues can be found in the TCGA database. (C) The presence of LINC01977 in tumors and corresponding nearby tissues in the TCGA database. (D) An ROC curve was generated to evaluate the effectiveness of LINC01977 in detecting CRC tissues. (E,F) Investigation of the expression of LINC01977 in both CRC and normal tissues using the GEO database. (G) The expression of LINC01977 was collected in 38 pairs of CRC and neighboring tissues. **, P<0.01; ***, P<0.001. ns, no statistical significance; TCGA, The Cancer Genome Atlas; CRC, colorectal carcinoma; ROC, receiver operating characteristic; GEO, gene expression database.

of expression in multiple cancer types, including CRC (*Figure 1A*). Afterwards, we analyzed the LINC01977 level in 51 paracancerous samples and 619 CRC samples obtained from the TCGA-colon adenocarcinoma/rectal adenocarcinoma (COAD/READ) datasets. The analysis showed a notable rise in LINC01977 manifestation in CRC samples (*Figure 1B*). Likewise, we also noticed a significant variation in LINC01977 manifestation among 50 CRC

specimens and their corresponding paracancerous specimens (*Figure 1C*). We employed receiver operating characteristic (ROC) curve analysis to assess the potential of LINC01977 as a discriminative indicator for CRC tissues. The area under the curve (AUC) value for LINC01977 was computed as 0.966, suggesting its potential as a distinguishing molecule for CRC tissues (*Figure 1D*). Furthermore, the examination of the GEO datasets [GSE109454 (11) and GSE115856] further revealed that the LINC01977 level in CRC surpassed that observed in neighboring tissues (*Figure 1E,1F*). Additionally, we performed qPCR analysis on 38 paired samples of CRC and adjacent tissues, which verified that LINC01977 displayed noticeably increased expression in CRC tissues (*Figure 1G*).

Associations between LINC01977 expression and clinicopathologic variables in CRC

To examine the correlation between LINC01977 expression and clinical characteristics, we employed the Kruskal-Wallis test and Wilcoxon rank sum test. The findings demonstrated that no significant correlations were observed with T stage (*Figure 2A*), whereas a robust association between elevated LINC01977 expression and unfavorable indicators such as advanced N stage (*Figure 2B*), M stage (*Figure 2C*), pathological stage (*Figure 2D*), lymphatic invasion (*Figure 2E*), and carcinoembryonic antigen (CEA) level (*Figure 2F*), However, no significant correlations were observed with degree of differentiation or neural invasion. Besides, as shown in Figure S1A, the expression of LINC01977 in the patients identified with outcome measurements of complete response (CR) and partial response (PR) was lower than the patients identified with disease stability and progression (SD and PD). Further analyses of prognostic outcomes showed a significant correlation between high expression of LINC01977 and poor overall survival (OS), disease-specific survival (DSS), and progression-free interval (PFI) (*Figure 2G-2I*). Subgroup analysis of PFI found that patients with high expression of LINC01977 in the N0-1 subgroup had poorer PFI, whereas those in the N2 subgroup was meaningless (Figure S1B-S1C). In addition, in the stage II–IV subgroup, patients with high expression of LINC01977 had poorer PFI, whereas patients with high expression of LINC01977 in the stage I subgroup was meaningless (Figure S1D-S1E). The AUC values for 1-, 2-, and 5-year PFI were included, showcasing the predictive potential of LINC01977 for PFI based on time-dependent ROC analysis (Figure S1F). These results suggested a correlation between LINC01977 and tumor progression, as well as a negative prognosis.

LINC01977 promotes the tumorigenesis of CRC in vitro and in vivo

The level of LINC01977 expression in CRC cells was notably higher compared to that in normal control NCM460 cells (*Figure 3A*). For *in vitro* experiments, the SW620 cells with the highest levels of LINC01977 and the HCT116 cells with the lowest levels were chosen. To explore the impact of LINC01977 on CRC cell viability and mobility, we overexpressed LINC01977 in HCT116 cells and suppressed its expression in SW620 cells, and the qRT-PCR results confirmed the corresponding overexpression and knockdown efficiency (*Figure 3B,3C*). Cell proliferation was assessed using the CCK-8 assay, which revealed a significant increase in cell proliferation following the upregulation of LINC01977 in HCT116 cells. Conversely, the suppression of LINC01977 in SW620 cells led to a significant decrease in cell proliferation (*Figure 3D*). Consistent results were also obtained through the colony formation assay (*Figure 3E*). To further assess the impact of LINC01977 on CRC tumorigenesis *in vivo*, we developed xenograft models. Remarkably, LINC01977 overexpression enhanced the growth of subcutaneous xenograft tumors, as did tumor weight (*Figure 3F*). Conversely, the LINC01977 knockdown group displayed a significant reduction in both tumor volume and weight (*Figure 3G*). Overall, these findings demonstrated that LINC01977 promoted the tumorigenesis of CRC.

LINC01977 promotes CRC metastasis in vitro and in vivo

Scratch and transwell assays were performed to clarify the role of LINC01977 in the mobility of CRC cells. During the scratch assays, we noticed a notable rise in the movement of HCT116 cells when LINC01977 was upregulated (*Figure 4A*), whereas the migration in SW620 cells decreased upon the downregulation of LINC01977 (*Figure 4B*). In the same way, transwell migration tests showed a higher quantity of migrating HCT116 cells after LINC01977 overexpression (*Figure 4C*), whereas SW620 cell migration decreased after LINC01977 knockdown (*Figure 4D*). Furthermore, the transwell invasion assays demonstrated that enhancing the expression of LINC01977 strengthened the invasion ability of HCT116 cells (*Figure 4E*), whereas reducing its expression impeded the

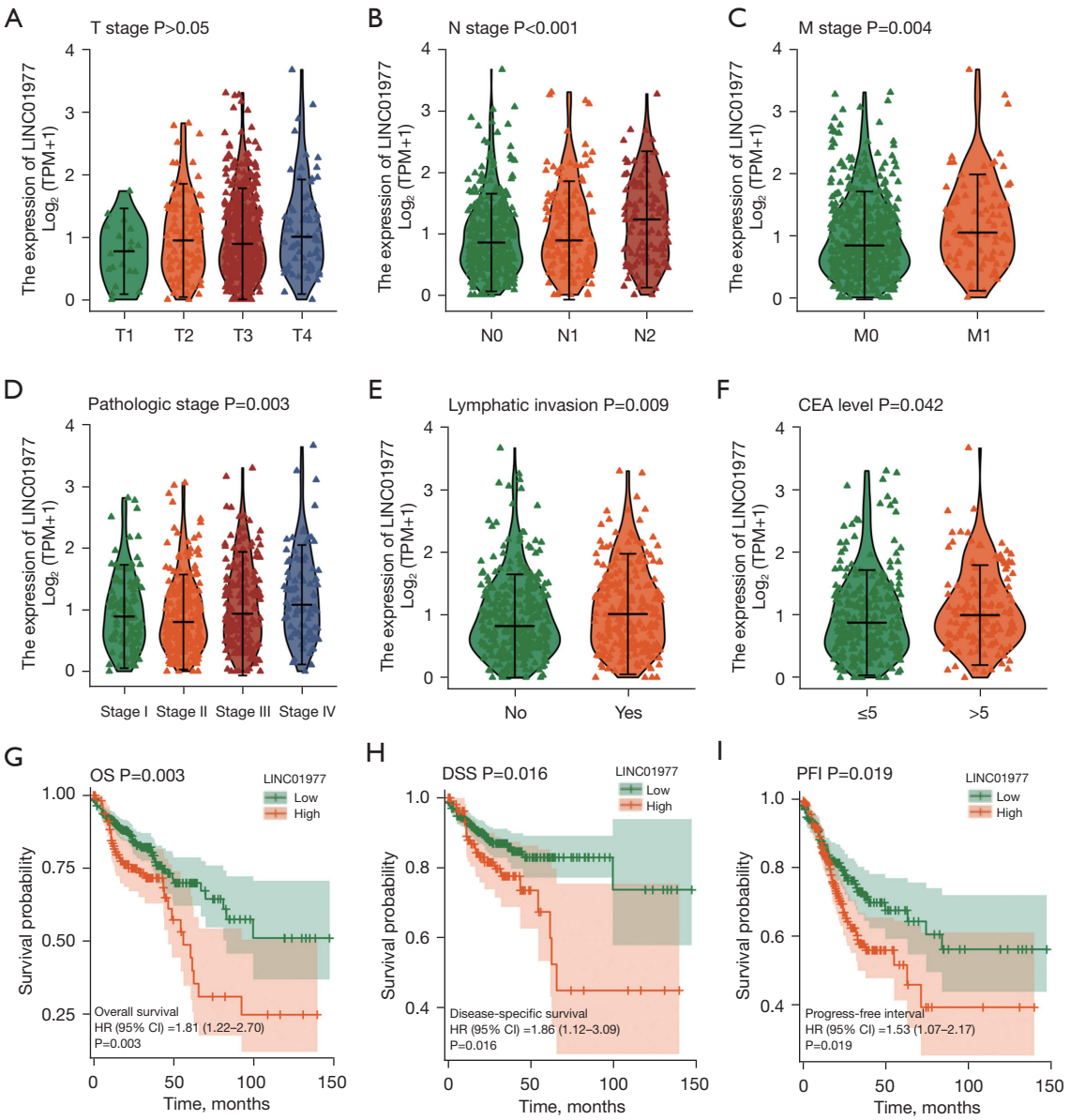

Figure 2 Association of LINC01977 expression with clinicopathologic characteristics and the survival curves in CRC patients in TCGA cohort. (A) Tumor stage; (B) lymph node stage; (C) metastasis stage; (D) stage determined by pathology; (E) presence of lymphatic invasion; (F) level of CEA; (G-I) Survival curves comparing OS, DSS, and PFI in patients with CRC categorized as LINC01977-high and LINC01977-low. OS, overall survival; DSS, disease-specific survival; PFI, progression-free interval; CRC, colorectal cancer.

invasion of SW620 cells (*Figure 4F*). In order to obtain additional understanding regarding the influence of LINC01977 on CRC metastasis *in vivo*, we created models of lung metastasis and measured the number of metastatic nodules in the lungs. Significantly, the overexpression of LINC01977 resulted in a higher count of metastatic pulmonary nodules in comparison to the control group (*Figure 4G*), whereas the knockdown of LINC01977 led to a decrease in the number of metastatic pulmonary nodules (*Figure 4H*). When considered collectively, these discoveries offer convincing proof that LINC01977 plays a crucial role in CRC metastasis.

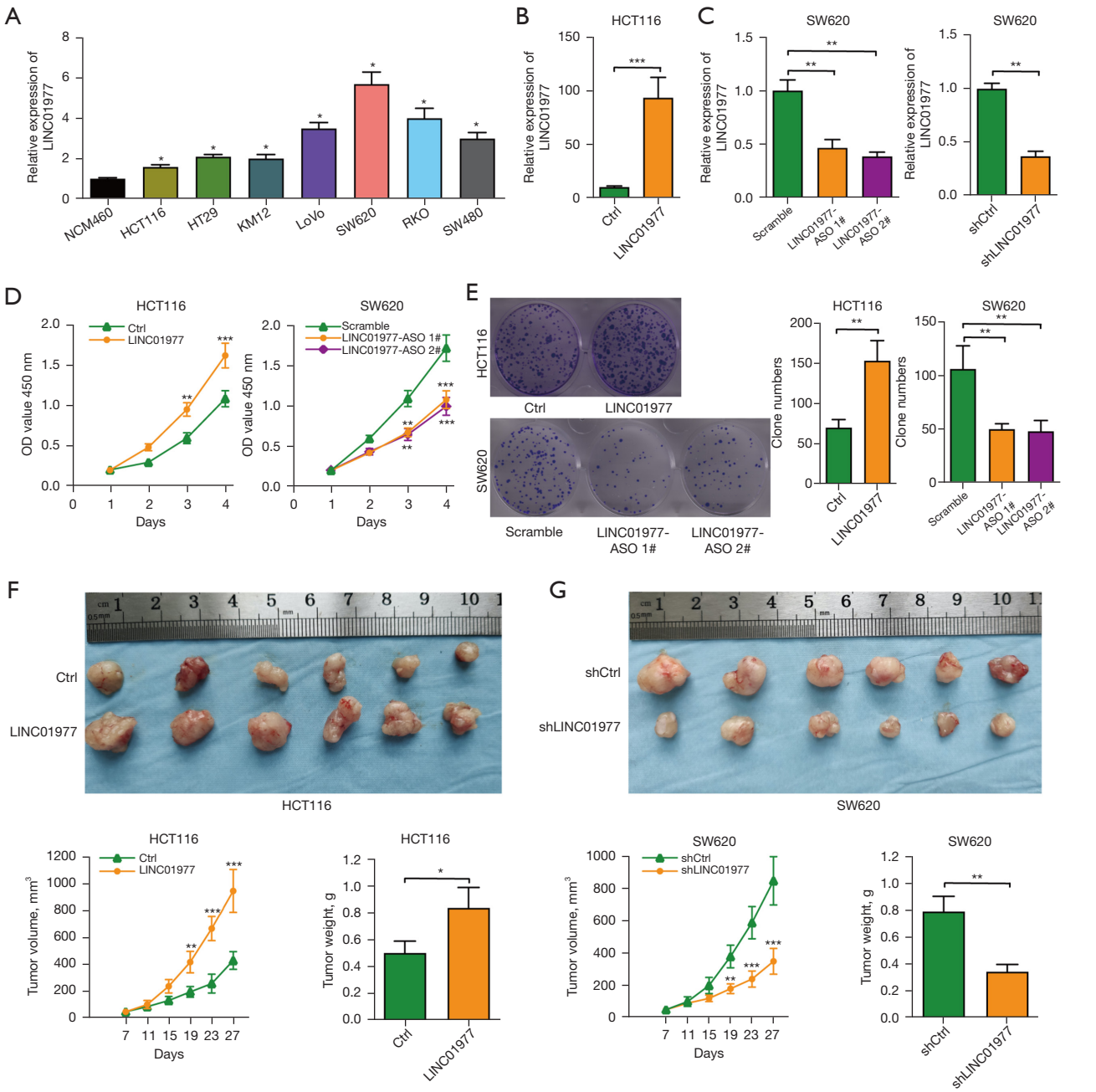

Figure 3 In both *in vitro* and *in vivo* settings, LINC01977 enhanced the growth of CRC cells. (A) The expression of LINC01977 in the CRC cell lines were identified by qRT-PCR with the normal colon epithelial cell line NCM460 serving as a control. (B) Following the upregulation of LINC01977 in HCT116 cell lines, the overexpression efficiency was confirmed using qRT-PCR. (C) Following the downregulation of LINC01977 in SW620 cell lines, the interference efficiency was confirmed using qRT-PCR. (D) CCK-8 assays and (E) colony formation assays revealed that upregulation of LINC01977 accelerated, whereas LINC01977 downregulation inhibited CRC cells proliferation. (F) Representative images of tumors derived from HCT116 cells with or without LINC01977 overexpression. Overexpressed LINC01977 enhanced the growth and weight of subcutaneous xenograft tumors. (G) Representative images of tumors derived from SW620 cells with or without LINC01977 knockdown. LINC01977 knockdown depressed the growth and weight of subcutaneous xenograft tumors. *, P<0.05; **, P<0.01; ***, P<0.001. qRT-PCR, quantitative real-time polymerase chain reaction; CRC, colorectal cancer; CCK-8, cell counting kit-8; OD, optical density.

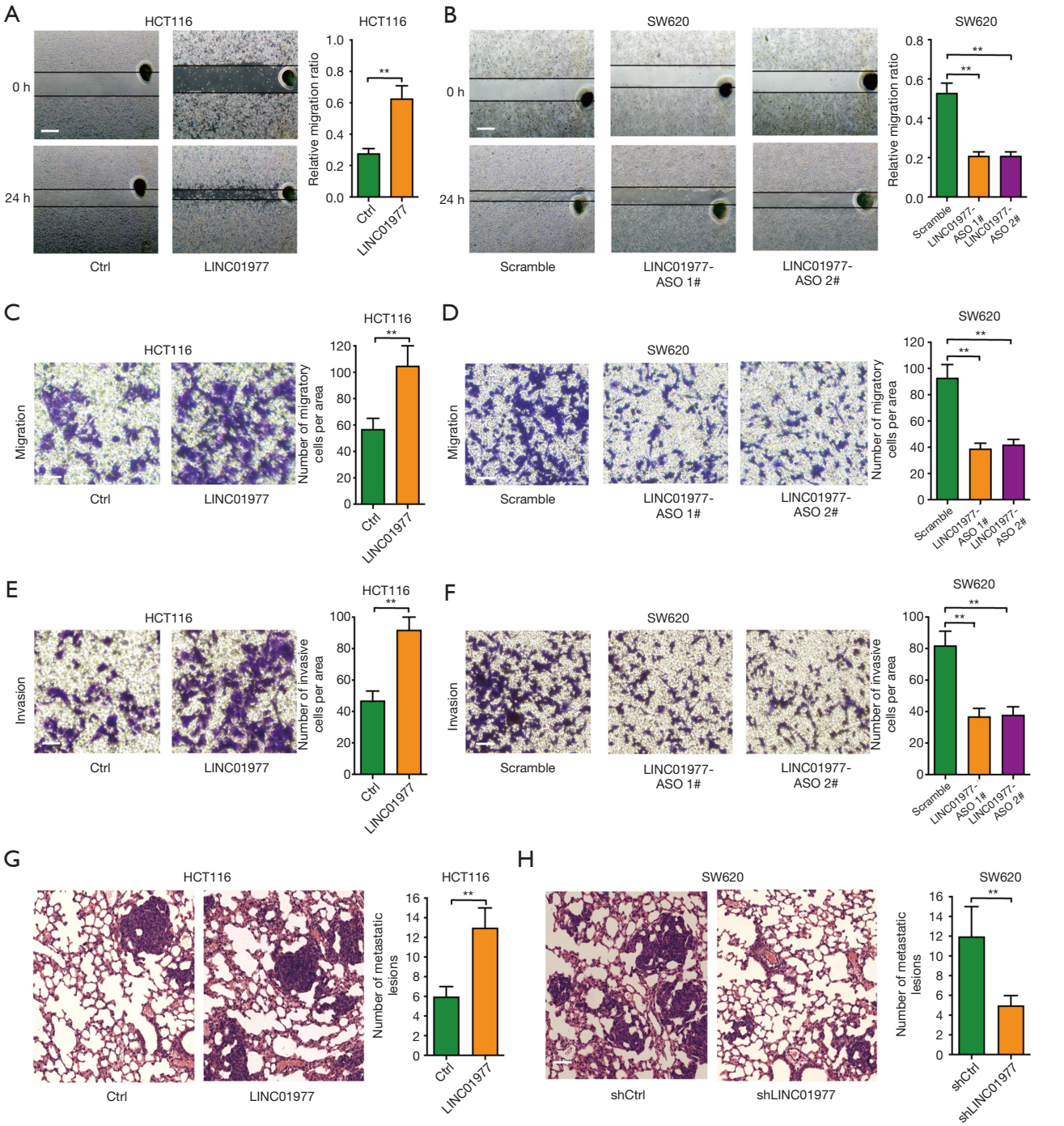

Figure 4 LINC01977 promoted metastasis of CRC *in vitro* and *in vivo*. (A,B) Scratch and (C,D) transwell migration assays demonstrated that the upregulation of LINC01977 enhanced, whereas the downregulation of LINC01977 reduced the migration of CRC cells, and cells in transwell assays were stained with 0.1% crystal violet. (E,F) Transwell invasion assays demonstrated that the upregulation of LINC01977 augmented the invasion of CRC cells, whereas the downregulation of LINC01977 reduced it, and cells in transwell assays were stained with 0.1% crystal violet. (G) The overexpression of LINC01977 resulted in a higher quantity of metastatic nodules in the lungs compared to the control group (H&E staining). (H) Knocking down LINC01977 led to a decrease in the quantity of metastatic nodules in the lungs (H&E staining). (The scale bar for the wound healing assay is 50 μm; that for the transwell assay is 100 μm; that for metastatic pulmonary nodules is 50 μm). **, P<0.01. CRC, colorectal cancer; H&E, hematoxylin and eosin.

LINC01977 modulates aerobic glycolysis in CRC

As it is commonly known, tumor cells rely on aerobic glycolysis to supply of nutrition and energy. Consequently, we proceeded to investigate whether LINC01977 could modulate glucose metabolism in CRC cells. The findings revealed that the overexpression of LINC01977 led to an augmentation in glucose uptake and lactate levels in HCT116 cells, compared to the corresponding control cells. Meanwhile, knockdown of LINC01977 resulted in a reduction in glucose uptake and lactate levels in SW620 cells (*Figure 5A*,*5B*). ECAR measurements were performed to further establish the role of LINC01977 in aerobic glycolysis. The results corroborated that overexpressing LINC01977 enhanced the glycolytic capacity and abilities of CRC cells (*Figure 5C*,*5D*), whereas silencing LINC01977 hindered their glycolytic potential (*Figure 5E*,*5F*). Additionally, the messenger RNA (mRNA) expression of glycolysis-related genes, such as *HK2*, *PGK1*, *LDHA*, and *GLUT1* were measured. The results demonstrated a decrease in the expression of these metabolic enzymes following LINC01977 knockdown (*Figure 5G*). Western blot analysis confirmed an increase in the expression of these metabolic enzymes upon LINC01977 overexpression, whereas a decrease was observed after LINC01977 knockdown (*Figure 5H*). Therefore, these data indicated that LINC01977 promoted aerobic glycolysis in CRC.

LINC01977 regulated CRC progression via c-Myc

In order to gain further insights into the underlying mechanism through which promotes the progression of CRC, we employed western blot analysis to examine the phosphorylation and protein levels of total extracellular signal-regulated kinase (ERK) and c-Myc in CRC cells following the overexpression and knockdown of LINC01977. The level of dually phosphorylated ERK1/2 (p-ERK1/2) was used to measure ERK1/2 activation. Our research uncovered that LINC01977 is capable of augmenting ERK1/2 phosphorylation and triggering ERK1/2 activation (*Figure 6A*). Given that ERK phosphorylates Ser62 of c-Myc and stabilizes it, we assessed the alterations in Ser62-phosphorylated c-Myc. In LINC01977-overexpressing cells, western blot analyses using pS62-cMyc antibody disclosed an elevation in phospho-S62 c-Myc and upregulation of c-Myc in CRC cells, whereas in the LINC01977 knockdown cells, the opposite effects were observed, suggesting that LINC01977 could regulate c-Myc stability through ERK-mediated phosphorylation (*Figure 6A*). Additionally, CCK-8 assays revealed that decreased expression of LINC01977 resulted in reduced proliferation, which could be reversed by overexpressing c-Myc (*Figure 6B*). Analysis of glucose intake revealed that c-Myc mitigated the reduction in glucose lactate brought about by the suppression of LINC01977 expression (*Figure 6C*). Observations from the lactate generation measurements showed that c-Myc curbed the decrease in lactate secretion triggered by the downregulation of LINC01977 expression (*Figure 6D*). Moreover, transwell assays unveiled that the dampened migration and invasion impacts exerted by LINC01977 downregulation on CRC cells could be countered by an upregulation of c-Myc (*Figure 6E-6H*). Thus, these results indicated that LINC01977 promoted proliferation, metastasis, and aerobic glycolysis of CRC cells through c-Myc.

Discussion

Numerous studies have identified dysregulated lncRNAs that contribute to CRC pathogenesis, including tumor initiation, growth, metastasis and therapy resistance. Increasing evidence supports that lncRNAs perform crucial functions in the development of CRC and possess considerable value for diagnostic and therapeutic approaches (12). Although the function of LINC01977 in CRC is still unclear, it has been reported to be involved in the advancement of lung adenocarcinoma through the TGF-β/SMAD3 pathway. Additionally, patients with early-stage lung adenocarcinoma displaying elevated expression levels of LINC01977 tend to have a shorter disease-free survival period (8). Another study demonstrated that LINC01977 not only significantly promoted the progression of breast cancer but also contributed to resistance against doxorubicin (9). Furthermore, LINC01977 exhibited high expression in hepatocellular carcinoma, and its overexpression was associated with poor OS of patients. LINC01977 interacted with RBM39 and facilitated the growth and metastasis of hepatocellular carcinoma by inhibiting Notch2 ubiquitination and degradation (10). In this study, we discovered that LINC01977 exhibited significantly elevated expression in CRC, and its expression correlated positively with unfavorable clinicopathological factors in CRC. Moreover, patients with higher levels of LINC01977 had worse prognosis. Subsequently, we investigated the impact of LINC01977 on cell proliferation

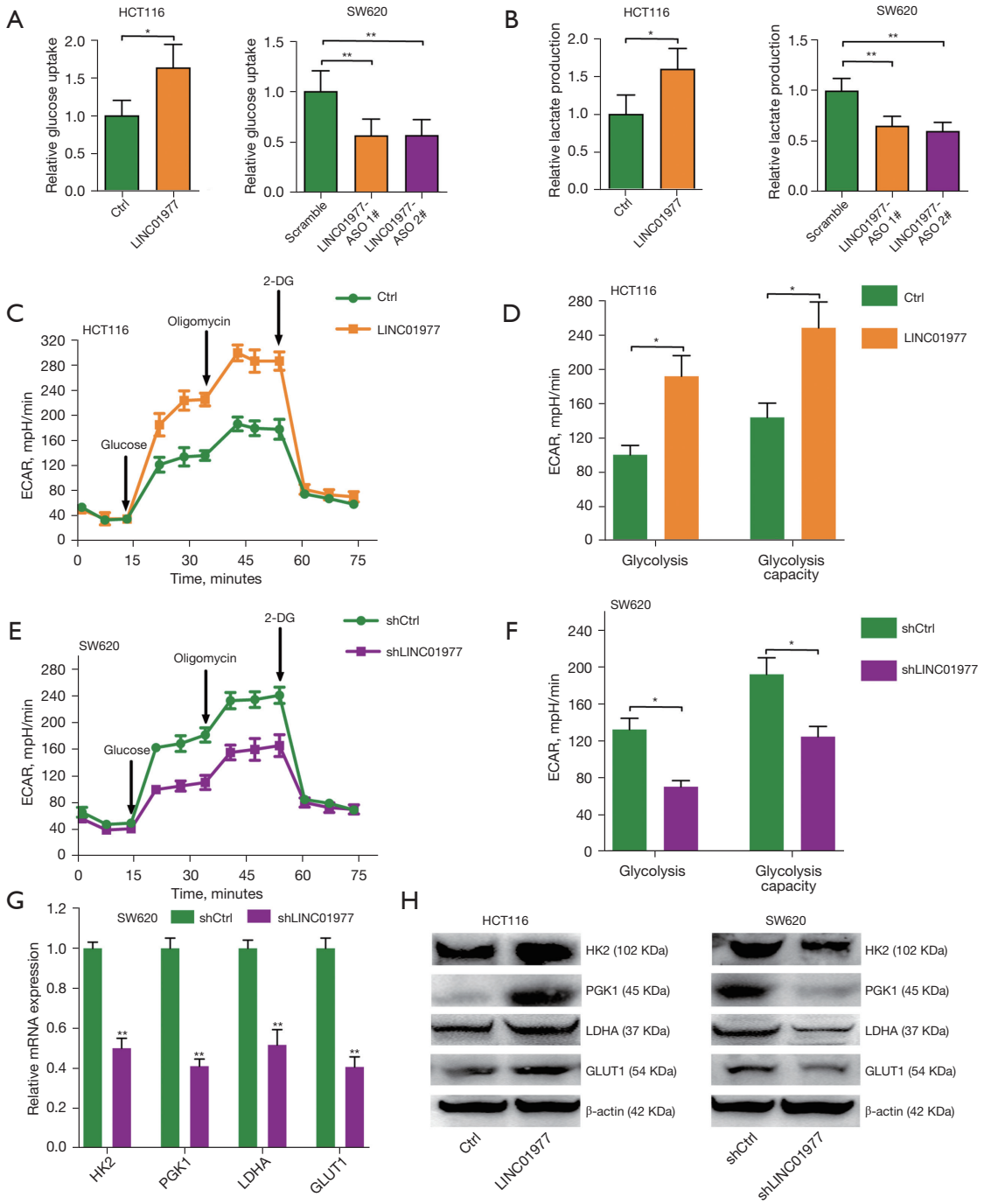

Figure 5 LINC01977 acts as a controller of aerobic glycolysis in CRC. (A) The results of the glucose uptake assay indicated that LINC01977 overexpression enhanced the capacity for glucose uptake, whereas LINC01977 knockdown reduced the capacity for glucose intake. (B) The results of the lactate level test showed that there was an elevation in lactate levels when LINC01977 was upregulated, whereas there was a reduction in lactate levels when LINC01977 was suppressed. (C,D) ECAR measurements showed that elevated LINC01977 expression led to enhanced glycolysis and glycolytic capacity in CRC cells. (E,F) ECAR measurements showed that reduced LINC01977 expression led to a decline in both glycolysis and glycolytic capacity in CRC cells. (G) qRT-PCR detected genes associated with glycolysis when LINC01977 was suppressed. (H) The enzyme-associated protein levels were evaluated upon overexpression or downregulation of LINC01977. *, P<0.05; **, P<0.01. CRC, colorectal cancer; ECAR, extracellular acidification rate; qRT-PCR, quantitative real-time polymerase chain reaction.

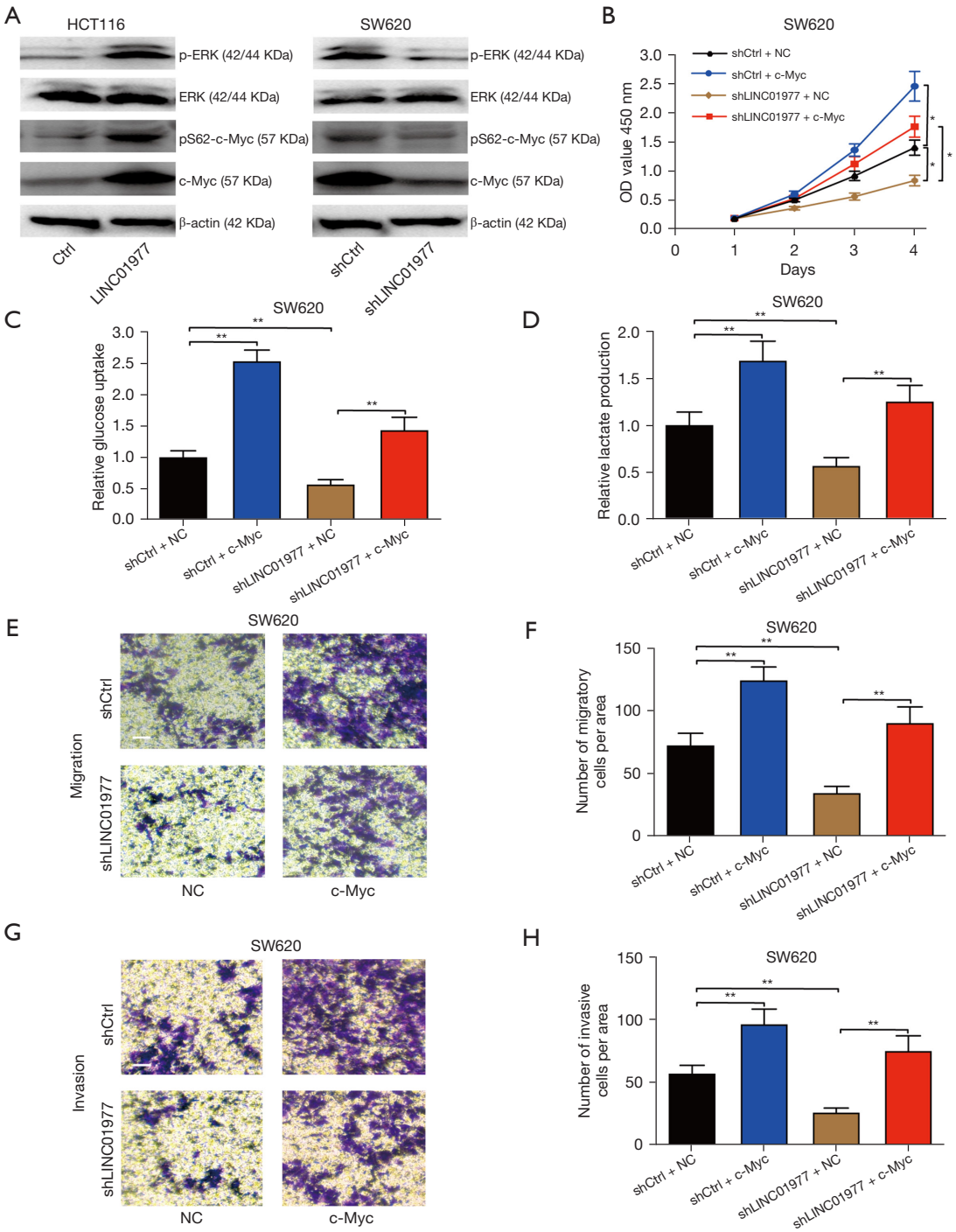

Figure 6 LINC01977 regulated aerobic glycolysis, proliferation, and metastasis of CRC cells through the regulation of c-Myc. (A) The protein levels of p-ERK, ERK, pS62-c-Myc, and c-Myc were assessed when LINC01977 was overexpressed or downregulated. (B) CCK-8 assays revealed that LINC01977 knockdown caused proliferation decreased could be reversed by c-Myc. (C) The analysis of glucose intake showed that c-Myc attenuated the decrease in glucose lactate resulting from the down-regulation of LINC01977. (D) The measurement of lactate production showed that c-Myc alleviated the decrease in lactate release caused by the down-regulation of LINC01977. (E-H) The migration and invasion effects of LINC01977 on CRC cells, which were reduced, could be restored by c-Myc, as shown by transwell assays, in which cells were stained with 0.1% crystal violet. (The scale bar for the transwell assay is 100 μm). *, P<0.05; **, P<0.01. CRC, colorectal cancer; CCK-8, cell counting kit-8; OD, optical density.

and metastasis of CRC through gain- and loss-of-function experiments. As anticipated, upregulated LINC01977 promoted cell proliferation and metastasis, whereas silenced LINC01977 exerted contrary effects. These findings revealed the crucial roles played by LINC01977 in the progression of CRC.

The role of enhanced aerobic glycolysis in accelerating uncontrolled proliferation of cancer cells is well-established. In CRC, aerobic glycolysis not only supplies nutrients for cell proliferation but also plays a regulatory role in metastasis, angiogenesis, cell differentiation and chemotherapy resistance (13-18). Hence, we further explored whether LINC01977 functioned as a regulator of aerobic glycolysis; the results revealed that LINC01977 facilitated aerobic glycolysis of CRC. With an aim to uncover the underlying mechanism, we investigated LINC01977's effect on c-Myc, which has been demonstrated to be a regulator in metabolism of malignancies. It can elevate tumor metabolism to meet the heightened energy demands associated with rapid tumor growth (19,20). Through the elevation of key glycolytic genes such as *HK2*, *PGK1*, *LDHA*, and *GLUT1*, c-Myc exerts control over aerobic glycolysis (21-26). Besides, researchers have shown that the activation of ERK results in an increase in c-Myc protein stability and levels through post translational phosphorylation and ubiquitination (27). Hence, the activation of ERK can enhance aerobic glycolysis by modulating c-Myc (28,29). In our study, we confirmed that LINC01977 induced the activation of ERK and then regulated c-Myc stability and expression, consequently promoting the growth, metastasis, and aerobic glycolysis of CRC through c-Myc.

Taken together, this study identified LINC01977 as a novel prognostic marker for CRC survival. Mechanistic investigations revealed that LINC01977 performed important functions in promoting tumorigenesis and aerobic glycolysis in CRC through the regulation of c-Myc. The potential influence of LINC01977 on the progression and metastasis of CRC may play a role in informing the development of personalized therapeutic interventions. Assessing the expression levels of LINC01977 in individual patients may assist in determining optimal treatment approaches tailored to the expected disease aggressiveness. There is a possibility that LINC01977 could serve as a potential biomarker for patient risk stratification and local regional metastasis assessment. However, it should be noted that additional studies are needed to confirm the prognostic value of LINC01977 as a standalone biomarker or in combination with other established markers. The insights obtained from this research could aid in the development of novel therapeutic approaches for CRC.

Conclusions

To our knowledge, this research provides the first evidence on the clinical relevance and functional role of LINC01977 in CRC. Our findings indicate that LINC01977 plays a significant part in enhancing the growth, metastasis, and aerobic glycolysis of CRC via c-Myc. Further investigations into the role of LINC01977 in CRC have the potential to unveil novel therapeutic targets and ultimately improve the prognosis for patients with CRC.

Acknowledgments

Funding: This work was supported by National Natural Science Foundation of China (No. 32270705), Beijing Hengji Health Management and Development Foundation (No. HJ-HX-ZLXD-202209-004), and Traditional Chinese Medicine Research Project of Shanghai Municipal Health Commission (No. 2020LZ006).

Footnote

Reporting Checklist: The authors have completed the ARRIVE and MDAR reporting checklists. Available at https://jgo.amegroups.com/article/view/10.21037/jgo-24-52/rc

Data Sharing Statement: Available at https://jgo.amegroups.com/article/view/10.21037/jgo-24-52/dss

Peer Review File: Available at https://jgo.amegroups.com/article/view/10.21037/jgo-24-52/prf

Conflicts of Interest: All authors have completed the ICMJE uniform disclosure form (available at https://jgo.amegroups.com/article/view/10.21037/jgo-24-52/coif). The authors have no conflicts of interest to declare.

Ethical Statement: The authors are accountable for all aspects of the work in ensuring that questions related to the accuracy or integrity of any part of the work are appropriately investigated and resolved. For human research, the study was conducted in accordance with the Declaration of Helsinki (as revised in 2013). The

study was approved by the Ethics Committee of the First Affiliated Hospital of Soochow University (No. 2022344) and informed consent was taken from all the patients. The animal experiments were performed under a project license (No. 2021243) granted by the Animal Ethics Committee of the First Affiliated Hospital of Soochow University, in compliance with Chinese National Standard (GBT35823-2018) for the care and use of animals.

References

1. Sung H, Ferlay J, Siegel RL, et al. Global Cancer Statistics 2020: GLOBOCAN Estimates of Incidence and Mortality Worldwide for 36 Cancers in 185 Countries. CA Cancer J Clin 2021;71:209-49.
2. Siegel RL, Miller KD, Goding Sauer A, et al. Colorectal cancer statistics, 2020. CA Cancer J Clin 2020;70:145-64.
3. Dekker E, Tanis PJ, Vleugels JLA, et al. Colorectal cancer. Lancet 2019;394:1467-80.
4. Chen S, Shen X. Long noncoding RNAs: functions and mechanisms in colon cancer. Mol Cancer 2020;19:167.
5. Ghafouri-Fard S, Hussen BM, Gharebaghi A, et al. LncRNA signature in colorectal cancer. Pathol Res Pract 2021;222:153432.
6. Sarraf JS, Puty TC, da Silva EM, et al. Noncoding RNAs and Colorectal Cancer: A General Overview. Microrna 2020;9:336-45.
7. Zhang Z, Wu Y, Yu C, et al. Comprehensive analysis of immune related lncRNAs in the tumor microenvironment of stage II-III colorectal cancer. J Gastrointest Oncol 2021;12:2232-43.
8. Zhang T, Xia W, Song X, et al. Super-enhancer hijacking LINC01977 promotes malignancy of early-stage lung adenocarcinoma addicted to the canonical TGF-β/SMAD3 pathway. J Hematol Oncol 2022;15:114.
9. Li Z, Li Y, Wang X, et al. LINC01977 Promotes Breast Cancer Progression and Chemoresistance to Doxorubicin by Targeting miR-212-3p/GOLM1 Axis. Front Oncol 2021;11:657094.
10. Xia A, Yue Q, Zhu M, et al. The cancer-testis lncRNA LINC01977 promotes HCC progression by interacting with RBM39 to prevent Notch2 ubiquitination. Cell Death Discov 2023;9:169.
11. He F, Song Z, Chen H, et al. Long noncoding RNA PVT1-214 promotes proliferation and invasion of colorectal cancer by stabilizing Lin28 and interacting with miR-128. Oncogene 2019;38:164-79.
12. Yang Y, Yan X, Li X, et al. Long non-coding RNAs in colorectal cancer: Novel oncogenic mechanisms and promising clinical applications. Cancer Lett 2021;504:67-80.
13. Yu S, Zang W, Qiu Y, et al. Deubiquitinase OTUB2 exacerbates the progression of colorectal cancer by promoting PKM2 activity and glycolysis. Oncogene 2022;41:46-56.
14. Wu H, Du J, Li C, et al. Kaempferol Can Reverse the 5-Fu Resistance of Colorectal Cancer Cells by Inhibiting PKM2-Mediated Glycolysis. Int J Mol Sci 2022;23:3544.
15. Hu J, Feng L, Ren M, et al. Colorectal Cancer Cell Differentiation Is Dependent on the Repression of Aerobic Glycolysis by NDRG2-TXNIP Axis. Dig Dis Sci 2022;67:3763-72.
16. Deng F, Zhou R, Lin C, et al. Tumor-secreted dickkopf2 accelerates aerobic glycolysis and promotes angiogenesis in colorectal cancer. Theranostics 2019;9:1001-14.
17. Gu M, Zhou X, Sohn JH, et al. NF-κB-inducing kinase maintains T cell metabolic fitness in antitumor immunity. Nat Immunol 2021;22:193-204. Erratum in: Nat Immunol 2021;22:530.
18. Zhan L, Su F, Li Q, et al. Phytochemicals targeting glycolysis in colorectal cancer therapy: effects and mechanisms of action. Front Pharmacol 2023;14:1257450.
19. Hsieh AL, Walton ZE, Altman BJ, et al. MYC and metabolism on the path to cancer. Semin Cell Dev Biol 2015;43:11-21.
20. Stine ZE, Walton ZE, Altman BJ, et al. MYC, Metabolism, and Cancer. Cancer Discov 2015;5:1024-39.
21. Tang J, Yan T, Bao Y, et al. LncRNA GLCC1 promotes colorectal carcinogenesis and glucose metabolism by stabilizing c-Myc. Nat Commun 2019;10:3499.
22. Labak CM, Wang PY, Arora R, et al. Glucose transport: meeting the metabolic demands of cancer, and applications in glioblastoma treatment. Am J Cancer Res 2016;6:1599-608.
23. Shim H, Dolde C, Lewis BC, et al. c-Myc transactivation of LDH-A: implications for tumor metabolism and growth. Proc Natl Acad Sci U S A 1997;94:6658-63.

24. Sheng G, Gao Y, Ding Q, et al. P2RX7 promotes osteosarcoma progression and glucose metabolism by enhancing c-Myc stabilization. J Transl Med 2023;21:132.
25. Wu Y, Deng Y, Zhu J, et al. Pim1 promotes cell proliferation and regulates glycolysis via interaction with MYC in ovarian cancer. Onco Targets Ther 2018;11:6647-56.
26. Shi T, Ma Y, Cao L, et al. B7-H3 promotes aerobic glycolysis and chemoresistance in colorectal cancer cells by regulating HK2. Cell Death Dis 2019;10:308.
27. Ji S, Qin Y, Shi S, et al. ERK kinase phosphorylates and destabilizes the tumor suppressor FBW7 in pancreatic cancer. Cell Res 2015;25:561-73.
28. Qin Y, Hu Q, Ji S, et al. Homeodomain-interacting protein kinase 2 suppresses proliferation and aerobic glycolysis via ERK/cMyc axis in pancreatic cancer. Cell Prolif 2019;52:e12603.
29. Zhai S, Xu Z, Xie J, et al. Epigenetic silencing of LncRNA LINC00261 promotes c-myc-mediated aerobic glycolysis by regulating miR-222-3p/HIPK2/ERK axis and sequestering IGF2BP1. Oncogene 2021;40:277-91.

Cite this article as: Wu J, Chen Q, Wang Y, Wang R, Chen Q, Wang Y, Qi X, Gao Y, Chen K. LINC01977 promotes colorectal cancer growth and metastasis by enhancing aerobic glycolysis via the ERK/c-Myc axis. J Gastrointest Oncol 2024;15(1):271-285. doi: 10.21037/jgo-24-52

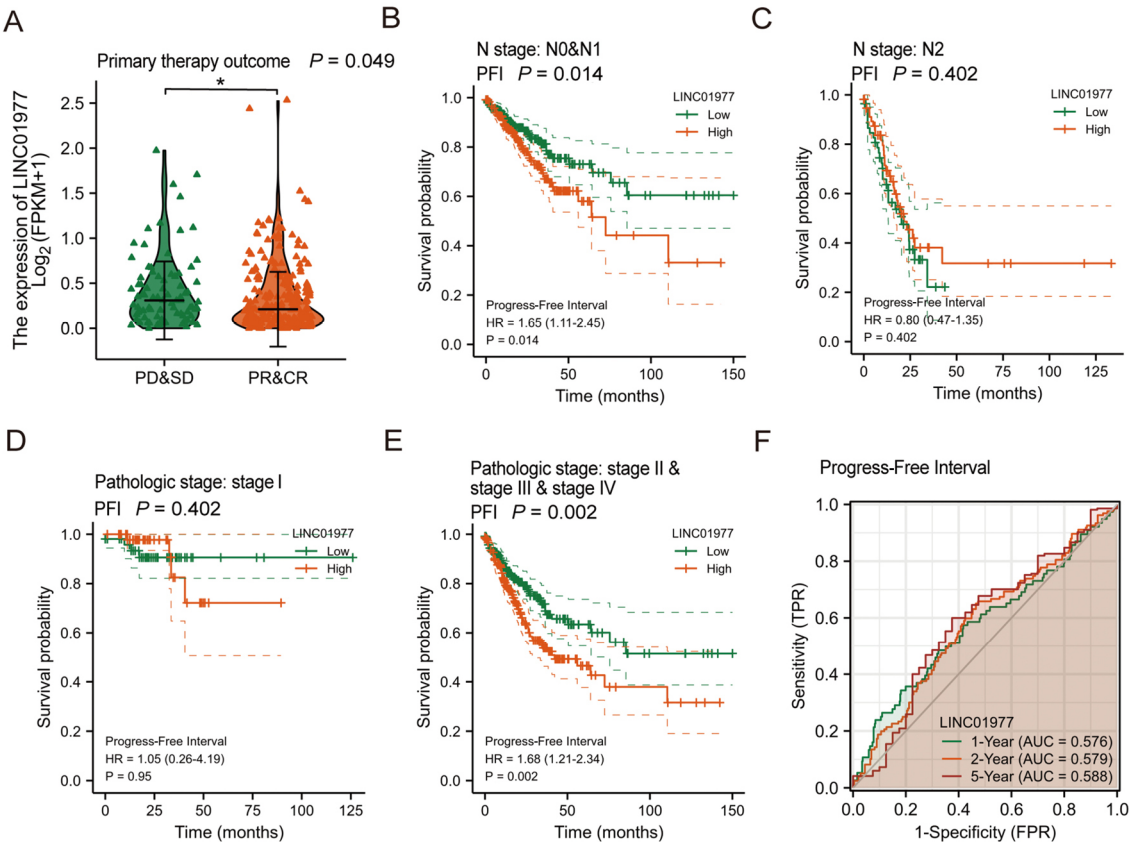

Figure S1 In the TCGA cohort, clinicopathologic characteristics and subgroup analysis of the survival curves of CRC patients were compared based on the high and low levels of LINC01977. (A) Association of LINC01977 expression with primary therapy outcome. (B,C) Survival curves of stage N0-1 and stage N2 subgroups in patients with CRC were compared based on LINC01977-high and LINC01977-low levels of PFI. (D,E) Survival curves of pathologic stage I and stage II–IV subgroups in patients with CRC were compared based on LINC01977-high and LINC01977-low levels of PFI. (F) The time-dependent ROC provided the area under the curve (AUC) for 1-, 2-, and 5-year PFI to assess the value of LINC01977. *, P<0.05. TCGA, The Cancer Genome Atlas; CRC, colorectal cancer; PFI, progression-free interval; ROC, receiver operating characteristic.

https://dx.doi.org/10.21037/jgo-24-52